Journal of Solid State Chemistry 184 (2011) 2083–2087

Contents lists available at ScienceDirect

Journal of Solid State Chemistry

journal homepage: www.elsevier.com/locate/jssc

Phase equilibria and crystal structure of the complex oxides in the *Ln*–Ba–Co–O (*Ln*=Nd, Sm) systems

L.Ya. Gavrilova, T.V. Aksenova, N.E. Volkova, A.S. Podzorova, V.A. Cherepanov*

Department of Chemistry, Ural State University, Ekaterinburg, Russia

ARTICLE INFO

Article history:
Received 26 March 2011
Received in revised form
3 June 2011
Accepted 6 June 2011
Available online 12 June 2011

Keywords:
Cobaltates
Phase equilibria
Crystal structure
Oxygen content

ABSTRACT

The phase equilibria in the *Ln*–Ba–Co–O (*Ln*=Nd, Sm) systems were systematically studied at 1100 °C in air. The homogeneity ranges and crystal structure of the solid solutions: $Ln_{2-x}Ba_xO_{3-\delta}$ ($0<x\le0.1$ for *Ln*=Nd and $0<x\le0.3$ for *Ln*=Sm), $Nd_{3-y}Ba_yCo_2O_7$ ($0.70\le y\le0.80$), $BaCo_{1-z}Sm_zO_{3-\delta}$ ($0.1\le z\le0.2$) were determined by X-ray diffraction of quenched samples. The values of oxygen content ($5+\delta$) for slowly cooled $LnBaCo_2O_{5+\delta}$ (*Ln*=Nd, Sm) samples were estimated as 5.73 for *Ln*=Nd, and 5.60 for *Ln*=Sm. The unit cell parameters were refined using Rietveld full-profile analysis. It was shown that $NdBaCo_2O_{5.73}$ possesses tetragonal structure and $SmBaCo_2O_{5.60}$ – orthorhombic structure. The projections of isothermal–isobaric phase diagrams for the *Ln*–Ba–Co–O (*Ln*=Nd, Sm) systems to the compositional triangle of metallic components were presented.

1. Introduction

Mixed rare earth (Nd, Sm) and barium cobaltates attract significant attention as promising electrode materials for intermediate-temperature solid oxide fuel cells [1–5]. The state-of-the-art research is mainly devoted to the preparation procedure, crystal structure, oxygen nonstoichiometry and physicochemical properties of so-called double perovskite phases $LnBaCo_2O_{5+\delta}$ [2–8]. On the contrary the phase equilibria of the *Ln*–Ba–Co–O systems (*Ln*=Nd, Sm), that corresponds to a physicochemical basis of every material, have not been systematically studied yet. More or less detailed information is available for the corresponding ternary systems.

In both *Ln*–Co–O (*Ln*=Nd, Sm) systems $LnCoO_{3-\delta}$ are the only phases formed at 1100 °C in air [9–14]. Both neodymium and samarium cobaltates possess orthorhombically distorted perovskite-type structure [15–17]. So-called Ruddlesden–Popper phases $Nd_4Co_3O_{10}$ and Nd_2CoO_4, where cobalt ions possesses lower oxidation states were prepared in more reducing conditions (lower oxygen partial pressure) [10,18–21].

Two complex oxides $BaCoO_{3-\delta}$ and Ba_2CoO_4 were described in the Ba–Co–O system earlier [22–25] existing in air at 1100 °C. Although there are a number of other phases in this system obtained at the lower temperature: members of the $A_{n+2}B'B_nO_{3n+3}$ homologous series synthesized at 920 °C [26] and members of the $(Ba_8Co_6O_{18})_\alpha$ $(Ba_8Co_8O_{24})_\beta$ series prepared within the temperature range 800–875 °C [27,28].

Complex oxides with general formula Ln_2BaO_4 that possess orthorhombic structure were formed in the *Ln*–Ba–O systems (*Ln*=Nd, Sm) [29–32]. It is also known that alkali earth metal oxides can be partially dissolved in the rare earth sesquioxides [33].

In the quasibinary $LnCoO_{3-\delta}$–$BaCoO_{3-\delta}$ (*Ln*=Nd, Sm) systems so-called double perovskites $LnBaCo_2O_{5+\delta}$ characterized by the ordering of cations (*Ln*, Ba) in A-sublattice and possible ordering of vacancies in oxygen sublattice were described earlier [2–8]. Depending on the size of rare earth metal and oxygen content these complex oxides crystallized either in tetragonal $a_p\times a_p\times 2a_p$ cell (space group *P4/mmm*, so-called "112"-structure), or in orthorhombic $a_p\times 2a_p\times 2a_p$ cell (space group *Pmmm*, so-called "122"-structure), where a_p is the cubic perovskite unit cell parameter. It was shown that double perovskites $LnBaCo_2O_{5+\delta}$ possess orthorhombic structure in vicinity of the value of oxygen content 5.5 (approximately 5.4–5.6), while outside this interval they are crystallized in tetragonal structure [7]. Such behavior is differing from the phase equilibrium in $LaCoO_{3-\delta}$–$BaCoO_{3-\delta}$ system [34,35], where a wide range of $La_{1-u}Ba_uCoO_{3-\delta}$ solid solutions ($0\le u\le0.8$) was found at 1100 °C in air.

Khalyavin et al. [36] found that partial substitution of neodymium by barium can take place and as a result $Nd_{1-u}Ba_uCoO_{3-\delta}$ solid solutions have formed up to $u=0.3$ at 1200 °C in air. On the contrary no homogeneity ranges had been found in the $SmCoO_{3-\delta}$–$BaCoO_{3-\delta}$ cross-section [36].

A new phase with $Sm_2BaCo_2O_{3-\delta}$ composition, prepared by solid state reaction at 1300 K in flowing oxygen for 2 weeks was reported by Siwen and Yufang [37]. Gillie et al. [38] could not

* Corresponding author.
E-mail address: Vladimir.Cherepanov@usu.ru (V.A. Cherepanov).

0022-4596/$ - see front matter © 2011 Elsevier Inc. All rights reserved.
doi:10.1016/j.jssc.2011.06.006

obtain single phase sample with $Sm_2BaCo_2O_{5-\delta}$ nominal composition at approximately same conditions but suggested that true composition was probably close to $Sm_{2.1}Ba_{0.8}Co_{2.1}O_{7-\delta}$ (where $\delta \approx 1$).

This paper focuses on the phase equilibria in the *Ln*–Ba–Co–O (*Ln*=Nd, Sm) systems at 1100 °C in air and the crystal structure of intermediate phases. Since crystal structure of the double perovskites $LnBaCo_2O_{5+\delta}$ strongly depends on the oxygen content the changes of δ as a function of temperature were measured.

2. Experimental

The samples were prepared using a conventional ceramic route and glycerin nitrate technique. In both methods rare earth oxides Nd_2O_3 and Sm_2O_3 (with 99.99% purity), $BaCO_3$ and Co_3O_4 (both of "pure for analysis" grade) and metallic cobalt were used as starting materials. Metallic cobalt was obtained by reducing of cobalt oxide in the hydrogen flow at 500–600 °C. Before weighting the starting materials (oxides and barium carbonate) were preliminary annealed in order to remove adsorbed gases and water. Solid state synthesis was performed by stages within the temperature range 850–1100 °C in air with intermediate grindings in the agate mortar in alcohol media. According to the glycerin nitrate technique rare earth oxides, barium carbonate and metallic cobalt taken in appropriate ratios were dissolved in nitric acid, and then glycerin in the amount needed for a complete reduction of nitrate ions was added. Following heating first led to the formation of viscous gel that subsequently transformed to brown powder. Finally this powder was annealed at 1100 °C during 120–240 h with intermediate grindings. All samples for the phase equilibria study were quenched to room temperature with cooling rate ~500°/min. The samples of double perovskites $LnBaCo_2O_{5+\delta}$ for the structural examination were slowly cooled from 1100 °C (cooling rate about 100 K/h) in air.

X-ray diffraction of quenched or slowly cooled powder samples were performed at room temperature using diffractometer DRON-UM1 in Cu-$K\alpha$ radiation with pyrolytic graphite monochromator within the angle range $10° \le 2\theta \le 70°$ (scan step 0.04° with the exposure time 5–10 s). Powder neutron profiles were measured at the research reactor IVV-2, located near Ekaterinburg, Russia, on the D7A diffractometer. The wavelength employed was 1.5155 Å. The structural parameters were refined by the Rietveld profile method using the Fullprof-2008 package.

The changes of oxygen content in the single phase complex oxides were measured by TGA method (STA 409PC, Netzsch Gmbh). The samples were placed in the TGA cell, heated up to 1100 °C and equilibrated in air at this temperature during 8 h. The measurements performed in the cooling/heating mode (cooling/heating rate 2 K/min) coincide with each other. The absolute values of oxygen content were determined using direct reduction of $LnBaCo_2O_{5+\delta}$ in hydrogen flow at 1100 °C inside the TGA cell according to the following reaction:

$$LnBaCo_2O_{5+\delta} + (2.5+\delta)H_2 \rightarrow \tfrac{1}{2}Ln_2O_3 + BaO + 2Co + (2.5+\delta)H_2O.$$

3. Results and discussion

3.1. Ln–Ba–O system

In order to check a possibility of partial dissolution of barium in Nd_2O_3 and Sm_2O_3 a number of samples with overall formula $Ln_{2-x}Ba_xO_{3-\delta}$ within the range $0.05 \le x \le 0.6$ were prepared at 1100 °C in air by ceramic and glycerin-nitrate techniques.

Table 1
Unit cell parameters and reliability factors (R_i)[a] for the $Ln_{2-x}Ba_xO_{3-\delta}$ (*Ln*=Nd, Sm) solid solutions.

x	a (Å)	b (Å)	c (Å)	V (Å)^3	R_{Br} (%)	R_f (%)	R_p (%)
$Nd_{2-x}Ba_xO_{3-\delta}$ space group $P\bar{3}m1$							
0.05	3.828(1)	3.828(1)	5.995(1)	76.10(1)	1.84	1.55	17.1
0.075	3.827(1)	3.827(1)	5.994(1)	76.07(1)	1.40	1.51	14.3
0.1	3.827(1)	3.827(1)	5.991(1)	76.02(2)	1.37	1.41	14.4
$Sm_{2-x}Ba_xO_{3-\delta}$ Space group $C2/m$							
0.05	14.191(1)	3.628(1)	8.860(1)	449.22(2)	1.27	1.15	10.2
0.1	14.180(1)	3.626(1)	8.855(1)	448.39(1)	3.20	2.45	13.9
0.2	14.177(1)	3.625(1)	8.853(1)	448.08(1)	2.40	2.21	13.7
0.3	14.175(1)	3.625(1)	8.851(1)	447.92(2)	1.82	2.01	13.3

[a] Here and in the next tables the reliability factors appears in the Rietveld analysis are: R_{Br}–Bragg factor; R_f–structural factor; R_p–profile factor.

According to the results of X-ray diffraction the homogeneity ranges for the $Ln_{2-x}Ba_xO_{3-\delta}$ solid solutions at studied conditions appears within $0 < x \le 0.1$ for *Ln*=Nd and $0 < x \le 0.3$ for *Ln*=Sm. The samples with larger values of barium content ($0.1 < x \le 0.6$ for *Ln*=Nd and $0.3 < x \le 0.6$ for *Ln*=Sm) consisted of the saturated solid solution ($Nd_{1.9}Ba_{0.1}O_{3-\delta}$ or $Sm_{1.7}Ba_{0.3}O_{3-\delta}$, respectively) and Ln_2BaO_4. Similarly to the parent rare earth oxide Ln_2O_3 their solid solution possesses the same crystal structure: $Nd_{2-x}Ba_xO_{3-\delta}$ crystallized in $P\bar{3}m1$ space group, and $Sm_{2-x}Ba_xO_{3-\delta}$ – in $C2/m$ sp. gr. The unit cell parameters refined by the Rietveld method are presented in Table 1.

3.2. $LnCoO_{3-\delta}$–$BaCoO_{3-\delta}$ system

In order to study the nature of phases existing within the range $Ln_{1-u}Ba_uCoO_{3-\delta}$ (u=0.0–1.0; *Ln*=Nd, Sm) the samples of appropriate compositions with the step 0.1 were prepared using standard ceramic and glycerin-nitrate techniques. According to the results of XRD the only intermediate phase formed in both systems was $LnBaCo_2O_{5+\delta}$ (u=0.5, *Ln*=Nd, Sm). The samples in the range $0 < u < 0.5$ consisted of $LnCoO_{3-\delta}$ and $LnBaCo_2O_{5+\delta}$, while in the range $0.5 < u < 1$ $LnBaCo_2O_{5+\delta}$ and $BaCoO_{3-\delta}$ coexisted. These results for Sm containing system are in good agreement with the conclusions made by Khalyavin et al. [36]. However an absence of barium solubility in $NdCoO_3$ in the present study (at least it has to be much less than 0.1) in contrast to the value of homogeneity range u=0.3, reported in [36] is probably caused by the differences in annealing temperatures (1100 °C in present study and 1200 °C in [36]).

The values of oxygen content for the slowly cooled samples at room temperature were estimated from the TGA results as $(5+\delta)$=5.73 for *Ln*=Nd, and $(5+\delta)$=5.60 for *Ln*=Sm. According to the results of XRD analysis $NdBaCo_2O_{5.73}$ was found to be tetragonal (space group: $P4/mmm$), and $SmBaCo_2O_{5.6}$—orthorhombic (Space group: $Pmmm$) that are in good agreement with general relationship between oxygen content and crystal structure presented earlier [7]. Since the tetragonal→orthorhombic transformation associates with the oxygen vacancies ordering the structure of $NdBaCo_2O_{5.73}$ was also examined by neutron diffraction analysis. Neutron diffraction pattern of tetragonal $NdBaCo_2O_{5.73}$ is shown in Fig. 1a and XRD pattern for orthorhombic $SmBaCo_2O_{5.6}$—in Fig. 1b. The results of the Rietveld refinement for both samples are presented in Tables 2 and 3.

3.3. $Ln_{3-y}Ba_yCo_2O_7$ system

Since earlier it was reported about the existence of $Sm_2BaCo_2O_7$ [37,38], we have checked the possibility of $Ln_{3-y}Ba_yCo_2O_7$ (*Ln*=Nd, Sm) phases formation at 1100 °C in air. Thereto the

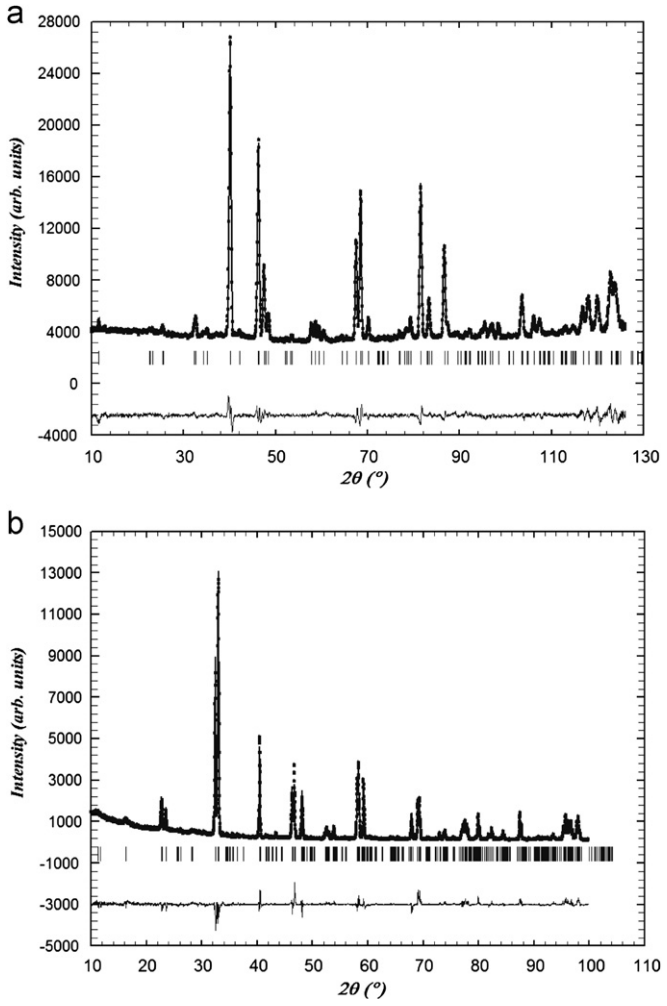

Fig. 1. Neutron diffraction pattern of $NdBaCo_2O_{5+\delta}$ oxide (a) and XRD pattern of $SmBaCo_2O_{5+\delta}$ oxide (b). Points represent the experimental data and the solid curve is the calculated profile. A difference curve is plotted at the bottom. Vertical marks represent the position of allowed Bragg reflections.

Table 2
Refined atomic coordinates, unit cell parameters and reliability factors for the $NdBaCo_2O_{5+\delta}$ oxide.

Space group *P4/mmm* $\delta=0.73$			
Atom	*x*	*y*	*z*
Nd	0.5	0.5	0.5
Ba	0.5	0.5	0
Co1	0	0	0.252(1)
O1	0	0	0
O2	0	0	0.5
O3	0	0.5	0.281(2)

$a=b=3.903(1)$; $c=7.614(1)$ Å; $V=116.02(2)$ (Å)^3; $R_{Br}=5.88\%$; $R_f=5.61\%$; $R_p=8.54\%$.

samples within the composition range $0.5 \le y \le 1.1$ with the step 0.05 were prepared using standard ceramic route and glycerin-nitrate technique described in Section 2. We failed to obtain $Sm_2BaCo_2O_7$, the sample of that nominal composition consisted of $SmBaCo_2O_{5+\delta}$ and $Sm_{2-x}Ba_xO_{3-\delta}$. On the contrary previously unknown phase in the $Nd_{3-y}Ba_yCo_2O_{7-\delta}$ series was detected within the composition range $0.7 \le y \le 0.8$. The samples prepared by ceramic technique after annealing at 1100 °C during 240 h besides

Table 3
Refined atomic coordinates, unit cell parameters and reliability factors for the $SmBaCo_2O_{5+\delta}$ oxide.

Space group *Pmmm* $\delta=0.60$			
Atom	*x*	*y*	*z*
Sm	0.5	0.229(3)	0.5
Ba	0.5	0.250(1)	0
Co1	0	0.5	0.255(2)
Co2	0	0	0.254(2)
O1	0	0	0
O2	0	0.5	0
O3	0	0.5	0.5
O4	0	0	0.5
O5	0.5	0	0.239(3)
O6	0.5	0.5	0.247(3)
O7	0	0.244(2)	0.238(2)

$a=3.886(1)$ Å; $b=7.833(1)$ Å; $c=7.560(1)$ Å; $V=230.22(2)$ (Å)^3; $R_{Br}=10.7\%$; $R_f=12.5\%$; $R_p=7.73\%$;

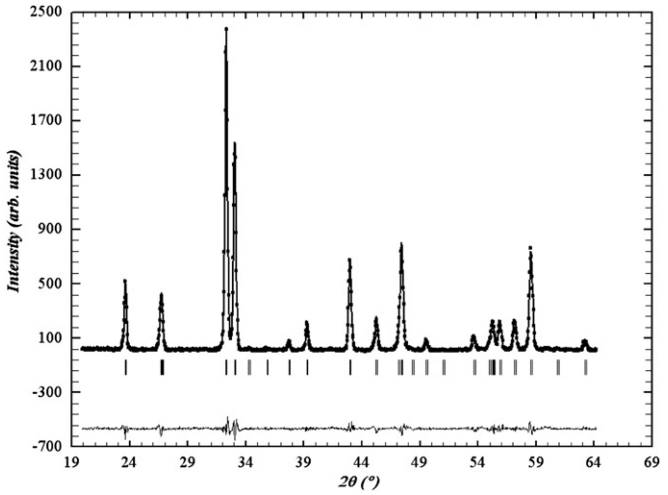

Fig. 2. XRD pattern of $Nd_{2.25}Ba_{0.75}Co_2O_{7-\delta}$ oxide. Points represent the experimental data and the solid curve is the calculated profile. A difference curve is plotted at the bottom. Vertical marks represent the position of allowed Bragg reflections.

Table 4
Unit cell parameters and reliability factors for the $Nd_{3-y}Ba_yCo_2O_{7-\delta}$ solid solutions.

Space group *I4/mmm*						
y	*a* (Å)	*c* (Å)	*V* (Å)^3	R_{Br} (%)	R_f (%)	R_p (%)
0.7	3.831(1)	20.015(2)	293.86(2)	0.974	0.712	9.68
0.75	3.833(1)	20.037(1)	294.34(3)	0.72	0.71	8.58
0.8	3.835(1)	20.069(2)	295.11(2)	1.96	1.90	13.3

the main phase contained small amount of $NdCoO_{3-\delta}$ и Nd_2O_3 as impurities. The samples obtained by glycerin-nitrate technique after 120 h annealing were single phase. XRD patterns of the single phase $Nd_{3-y}Ba_yCo_2O_7$ ($0.7 \le y \le 0.8$) samples were refined by Rietveld method within a tetragonal structure, *I4/mmm* space group. As an example, Fig. 2 illustrates XRD pattern for the $Nd_{2.25}Ba_{0.75}Co_2O_{7-\delta}$ oxide, and the values of structural parameters for all single phase samples are listed in Table 4.

3.4. Phase equilibria in the Ln–Ba–CO–O systems (Ln=Nd, Sm)

According to XRD patterns the samples enriched by (Sm+Ba) relatively to $Ln_{1-u}Ba_uCoO_{3-\delta}$ in the Sm–Ba–Co–O system contained

some previously unknown phase besides those described above. In order to explain an appearance of unknown phase a number of suppositions can be made. The first one is the possibility of stabilization of Ruddlesden–Popper type phases like $(Sm,Ba)_2CoO_4$. Furthermore Ba_2CoO_4 exist at studied conditions and possible substitution of Ba by Sm could not be excluding. In order to check this possibility a number of samples with nominal composition $(Ba_{1-u}Sm_u)_2CoO_4$ with the step $u=0.1$ were prepared. None of the samples annealed at 1100 °C during more than 200 h become single phase. Another supposition arises from the fact that the radius of samarium ion is much smaller than that of barium ion. Earlier it was shown that relatively small Y^{3+} can substitute Co ion rather than Ba forming $BaCo_{1-x}Y_xO_{3-y}$ [39]. No information concerning existence of $BaCo_{1-z}Ln_zO_{3-\delta}$ (Ln=Nd, Sm) had been found in the literature. A number of samples with nominal composition corresponding to the formula $BaCo_{1-z}Ln_zO_{3-\delta}$ were prepared for both (Sm and Nd) systems. All samples were equilibrated at 1100 °C during 200 h. As a result single phase samples $BaCo_{1-z}Sm_zO_{3-\delta}$ within the range $0.1 \le z \le 0.2$ were obtained. All single phase solid solutions possess cubic structure. XRD pattern for the single phase $BaCo_{0.85}Sm_{0.15}O_{3-\delta}$, as an example, is shown in Fig. 3, and unit cell parameters for all single phase samples are listed in Table 5. The sample with $z=0.05$ corresponds to a mixture of two phases: saturated solid solution $BaCo_{0.9}Sm_{0.1}O_{3-\delta}$ and hexagonal $BaCoO_{3-\delta}$. The samples with nominal composition $BaCo_{1-z}Nd_zO_{3-\delta}$ consisted of Nd_2BaO_4, $BaCoO_{3-\delta}$ and Ba_2CoO_4.

Overall phase equilibria in the Nd–Ba–Co–O system were analyzed based on the results of XRD of 63 quenched samples, and in the Sm–Ba–Co–O system – on 62 samples. Phase relations at fixed temperature and oxygen pressure in a quaternary system (Ln–Ba–Co–O) can be represented using a tetrahedron. A more convenient, planar representation can be obtained using the method of cross-sections. This method, however, is inapplicable to the system under consideration because the oxidation states of cobalt ions that various coexisted phases contain vary at the studied conditions, therefore the compositions of simple oxides and the compositions of the products do not lie in the same plane. For this reason, we used projection onto the plane of metallic components, an approach often used to represent such systems. In this respect the composition in the phase triangles is represented by the mole fraction of metallic components, for example $\xi_{Co}=(n_{Co}/n_{Ln}+n_{Ba}+n_{Co})$. The oxygen content of condensed phases in each point of a projection is assumed to be equal to the thermodynamically equilibrium value and could not be calculated from the composition triangle. The compositions of the samples taken into account are represented as points in the phase diagrams (Figs. 4 and 5). As a result the phase triangle for the Nd–Ba–Co–O system was divided into 12 fields (Fig. 4) and for the Sm–Ba–Co–O system – into 13 fields (Fig. 5).

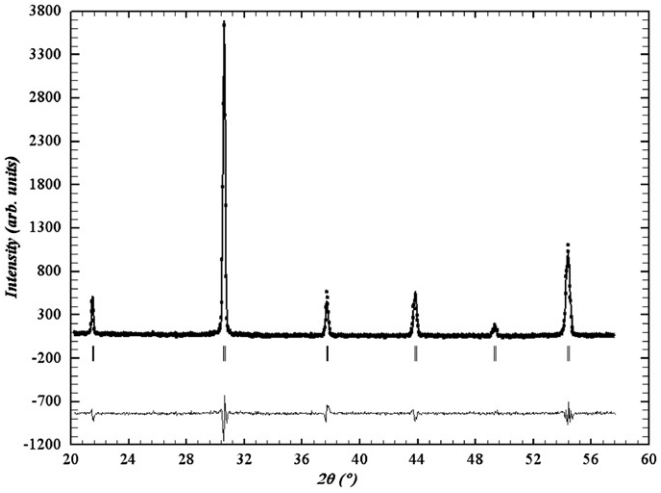

Fig. 3. XRD pattern of $BaCo_{0.85}Sm_{0.15}O_{3-\delta}$ oxide. Points represent the experimental data and the solid curve is the calculated profile. A difference curve is plotted at the bottom. Vertical marks represent the position of allowed Bragg reflections.

Table 5
Unit cell parameters and reliability factors for the $BaCo_{1-z}Sm_zO_{3-\delta}$ solid solutions.

z	a (Å)	V (Å)^3	R_{Br} (%)	R_f (%)	R_p (%)
0.1	4.108(1)	69.33(1)	2.04	1.72	13.4
0.15	4.131(1)	70.51(1)	1.59	1.50	9.76
0.2	4.143(1)	71.13(2)	1.30	1.09	16.4

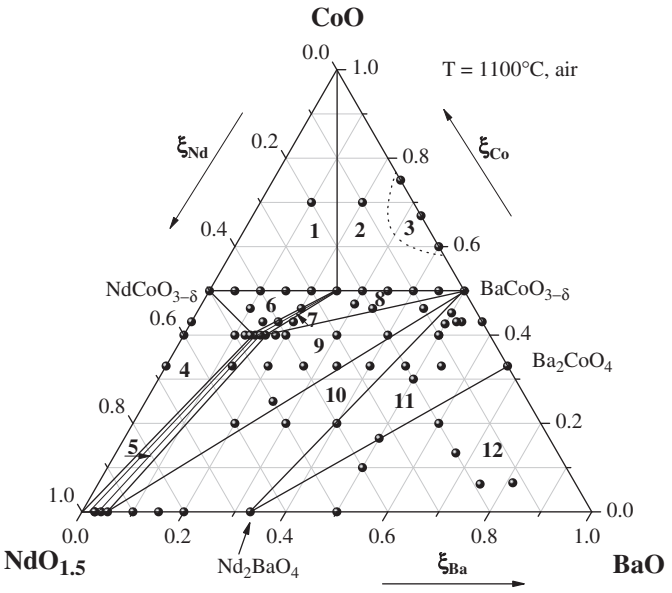

Fig. 4. A projection of isobaric isothermal phase diagram of the Nd–Ba–Co–O system to the metallic components triangle (T=1100 °C, Po_2=0.21 atm): 1–$NdCoO_{3-\delta}$, CoO and $NdBaCo_2O_{5+\delta}$; 2–CoO, $NdBaCo_2O_{5+\delta}$ and $BaCoO_{3-\delta}$; 3–melt; 4–Nd_2O_3, $NdCoO_{3-\delta}$ and $Nd_{2.3}Ba_{0.7}Co_2O_{7-\delta}$; 5–$Nd_{2-x}Ba_xO_{3-\delta}$ ($0 \le x \le 0.1$) and $Nd_{3-y}Ba_yCo_2O_{7-\delta}$ ($0.7 \le y \le 0.8$); 6–$NdCoO_{3-\delta}$, $NdBaCo_2O_{5+\delta}$ and $Nd_{2.3}Ba_{0.7}Co_2O_{7-\delta}$; 7–$NdBaCo_2O_{5+\delta}$ and $Nd_{3-y}Ba_yCo_2O_{7-\delta}$ ($0.7 \le y \le 0.8$); 8–$NdBaCo_2O_{5+\delta}$, $Nd_{2.2}Ba_{0.8}Co_2O_{7-\delta}$ and $BaCoO_{3-\delta}$; 9–$BaCoO_{3-\delta}$, $Nd_{2.2}Ba_{0.8}Co_2O_{7-\delta}$ and $Nd_{1.9}Ba_{0.1}O_{3-\delta}$; 10 – $BaCoO_{3-\delta}$, $Nd_{1.9}Ba_{0.1}O_{3-\delta}$ and Nd_2BaO_4; 11–$BaCoO_{3-\delta}$, Nd_2BaO_4 and Ba_2CoO_4; 12–Nd_2BaO_4, Ba_2CoO_4 and BaO.

It should be noted that similarly to the La–Ba–Co–O system [34,35] the melt regions (field 3 in Figs. 4 and 5) were detected in the vicinity of cobalt oxide content approximately 60–80% at CoO–BaO side for both Nd–Ba–Co–O and Sm–Ba–Co–O systems. Since no systematic study of melt regions has been performed in the present work these fields are shown schematically in the phase triangles.

4. Conclusion

The systematic study of phase equilibria in the Nd–Ba–Co–O and Sm–Ba–Co–O systems show the similarity in the compositional range $n_{Co}/(n_{Ln}+n_{Ba}) \ge 1$. In both systems the formation of so-called double perovskite $LnBaCo_2O_{5+\delta}$ takes place. However the difference in oxygen content in these complex oxides leads to the different crystal structure – tetragonal (space group $P4/mmm$) for $NdBaCo_2O_{5.73}$, and orthorhombic (space group $Pmmm$) for $SmBaCo_2O_{5.60}$. The phase equilibria in the compositional range $n_{Co}/(n_{Ln}+n_{Ba}) < 1$ differ significantly. The formation of $Nd_{3-y}Ba_yCo_2O_{7-\delta}$ solid solutions within the compositional range $0.7 \le y \le 0.8$ was detected in neodymium containing system and single phase $BaCo_{1-z}Sm_zO_{3-\delta}$ solid solutions were found to be

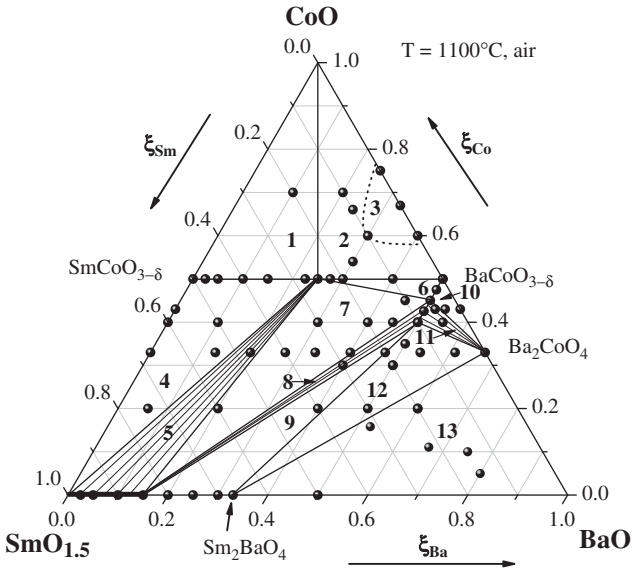

Fig. 5. A projection of isobaric isothermal phase diagram of the Sm–Ba–Co–O system to the metallic components triangle (T=1100 °C, Po_2=0.21 atm): 1–$SmCoO_{3-\delta}$, CoO and $SmBaCo_2O_{5+\delta}$; 2–CoO, $SmBaCo_2O_{5+\delta}$ and $BaCoO_{3-\delta}$; 3–melt; 4–Sm_2O_3, $SmCoO_{3-\delta}$ and $SmBaCo_2O_{5+\delta}$; 5–$SmBaCo_2O_{5+\delta}$ and $Sm_{2-x}Ba_xO_{3-\delta}$ ($0 \le x \le 0.3$); 6–$SmBaCo_2O_{5+\delta}$, $BaCoO_{3-\delta}$ and $BaCo_{0.9}Sm_{0.1}O_{3-\delta}$; 7–$SmBaCo_2O_{5+\delta}$, $BaCo_{0.9}Sm_{0.1}O_{3-\delta}$ and $Sm_{1.7}Ba_{0.3}O_{3-\delta}$; 8–$Sm_{1.7}Ba_{0.3}O_{3-\delta}$ and $BaCo_{1-z}Sm_zO_{3-\delta}$ ($0.1 \le z \le 0.2$); 9–$Sm_{1.7}Ba_{0.3}O_{3-\delta}$, Sm_2BaO_4 and $BaCo_{0.8}Sm_{0.2}O_{3-\delta}$; 10–$BaCoO_{3-\delta}$, Ba_2CoO_4 and $BaCo_{0.9}Sm_{0.1}O_{3-\delta}$; 11–$Ba_2CoO_4$ and $BaCo_{1-z}Sm_zO_{3-\delta}$ ($0.1 \le z \le 0.2$); 12–Sm_2BaO_4, Ba_2CoO_4 and $BaCo_{0.8}Sm_{0.2}O_{3-\delta}$; 13–$Sm_2BaO_4$, Ba_2CoO_4 and BaO.

stable within the range $0.1 \le z \le 0.2$ for the samarium containing system. Although the difference in the value of ionic radii of neodymium and samarium ions is not very large (Δr=0.03 Å [40]) they reveal different character of phase relations. Even their simple oxides crystallized in different space groups and homogeneity ranges of barium oxide solubility vary significantly ($0 < x \le 0.1$ for Nd and $0 < x \le 0.3$ for Sm).

Acknowledgments

This work was financially supported in parts by the Russian Foundation for Basic Research (project no. 09-03-00620) and the Ministry for Education and Science of the Russian Federation within the Federal Target Program "Research and Teaching Stuff of Innovative Russia for 2009–2013".

References

[1] E.V. Tsipis, V.V. Kharton, J. Solid State Electrochem. 12 (2008) 1367–1391.
[2] W. Zhou, T. He, Y. Ji, J. Power Sources 185 (2008) 754–758.
[3] E. Chavez, M. Mueller, L. Mogni, A. Caneiro, J. Appl. Phys.: Conf. Ser. 167 (2009) 012043.
[4] J.H. Kim, Y. Kim, P.A.C.J. Bae, W. Zhou, J. Power Sources 194 (2009) 704–711.
[5] J.-H. Kim, A. Manthiram, J. Electrochem. Soc. 155 (2008) B385–B390.
[6] A. Maignan, C. Martin, D. Pelloquin, N. Nguyen, B. Raveau, J. Solid State Chem. 142 (1999) 247–260.
[7] P.S. Anderson, C.A. Kirk, J. Knudsen, I.M. Reaney, A.R. West, Solid State Sci. 7 (2005) 1149–1156.
[8] T.V. Aksenova, L. Ya. Gavrilova, D.S. Tsvetkov, V.I. Voronin, V.A. Cherepanov, Russ. J. Phys. Chem. A 85 (2011) 427–432.
[9] A.N. Petrov, A.Yu. Kropanev, V.M. Zhukovskii, V.A. Cherepanov, G.K. Neudachina, Russ. J. Inorgan. Chem. 26 (1981) 3190–3194.
[10] A.N. Petrov, V.A. Cherepanov, A.Yu. Zuyev, V.M. Zhukovsky, J. Solid State Chem. 77 (1988) 1–14.
[11] A.Yu. Kropanev, A.N. Petrov, Inorgan. Mater. 19 (1983) 1782–1785.
[12] A.Yu. Kropanev, A.N. Petrov, V.M. Zhukovskii, Russ. J. Inorgan. Chem 28 (1983) 2938–2943.
[13] A.Yu. Kropanev, A.N. Petrov, L.Ya. Rabinovich, Russ. J. Inorgan. Chem. 28 (1983) 2609–2612.
[14] A.Yu. Kropanev, A.N. Petrov, L.Ya. Rabinovich, Inorgan. Mater. 20 (1984) 116–120.
[15] G. Demazeau, M. Pouchard, P. Hagenmuller, J. Solid State Chem. 9 (1974) 202–209.
[16] R. Flamand, R. Berjoan, High temperature-high pressures 15 (1983) 693–701.
[17] J.-P. Coutures, J.M. Badie, R. Berjoan, J. Coutures, R. Flamand, A. Rouanet, High Temp. Sci. 13 (1980) 331–336.
[18] K. Kitayama, J. Solid State Chem. 76 (1988) 241–247.
[19] K. Kitayama, J. Solid State Chem. 137 (1998) 255–260.
[20] A. Olafsen, H. Fjellvåg, B.C. Hauback, J. Solid State Chem. 151 (2000) 46–55.
[21] M.V. Kniga, I.I. Vygovskii, E.E. Klementovich, Zh. Neorgan. Khim. 24 (1979) 1171–1174.
[22] V.B. Lazarev, I.S. Shapligin, Izv. AN SSSR. Chem. Ser 14 (1982) 58–60.
[23] O.V. Godzhieva, N.V. Porotnikov, G.E. Nikiforova, Ye.A. Tishinko, Russ. J. Inorgan. Chem. 35 (1990) 44–48.
[24] A.J. Jacobson, J.L. Hutchison, J. Solid State Chem. 35 (1980) 334–340.
[25] K. Boulahya, M. Parras, A. Vegas, J.M. González-Calbet, Solid State Sci. 2 (2000) 57–64.
[26] K. Boulahya, M. Parras, J.M. González-Calbet, J. Solid State Chem. 142 (1999) 419–427.
[27] K. Boulahya, M. Parras, J.M. González-Calbet, Chem. Mater. 12 (2000) 2727–2735.
[28] J.M. González-Calbet, K. Boulahya, M.L. Ruiz, M. Parras, J. Solid State Chem. 162 (2001) 322–326.
[29] H. Kobayashi, H. Ogino, M. Nakamura, H. Yamamura, T. Mitamura, J. Ceram. Soc. Jpn. 102 (1994) 583–586.
[30] Q. Zhiyu, X. Xianran, Y. Wenxia, C. Xialong, W. Soukun, L. Jingkui, X. Sishen, J. Alloys Compd. 202 (1993) 77–80.
[31] R. Subasri, O.M. Sreedharan, J. Alloys Compd. 274 (1998) 153–156.
[32] Z.S. Vakhovskaya, A.L. Voskov, M.L. Kovba, I.A. Uspenskaya, J. Alloys Compd. (2006) 257–259408-412 (2006) 257–259.
[33] K.I. Portnoy, N.I. Timofeeva, Oxygen compounds of rare earth elements, Reference Book, Metallurgia, Moscow, 1986 in Russian.
[34] V.A. Cherepanov, L.Ya. Gavrilova, E.A. Filonova, M.V. Trifonova, V.I. Voronin, Mater. Res. Bull. 34 (1999) 983–988.
[35] V.A. Cherepanov, L.Ya. Gavrilova, L.Yu. Barkhatova, V.I. Voronin, M.V. Trifonova, O.A. Bukhner, Ionics 4 (1998) 309–315.
[36] D.D. Khalyavin, A.P. Sazonov, I.O. Troyanchuk, R. Szymczak, H. Szymczak, Inorg. Mater. 39 (2003) 1092–1096.
[37] L. Siwen, R. Yufang, J. Solid State Chem. 114 (1995) 286–288.
[38] L. Gillie, J. Hadermann, M. Hervieu, A. Maignan, C. Martin, Chem. Mater. 20 (2008) 6231–6237.
[39] M.V. Lomakov, S.Ya. Istomin, A.M. Abakumov, G. Van Tendeloo, E.V. Antipov, Solid State Ionics 179 (2008) 1885–1889.
[40] R.D. Shannon, Acta Crystallogr. A: Cryst. Phys. Diffr. Theor. Gen. Crystallogr. 32 (1976) 751–767.